

Use of Metabonomics to Identify Impaired Fatty Acid Metabolism as the Mechanism of a Drug-Induced Toxicity

Russell J. Mortishire-Smith,^{*,†} Gary L. Skiles,^{‡,§} Jeffrey W. Lawrence,[§]
Stan Spence,[§] Andrew W. Nicholls,^{||} Bruce A. Johnson,[⊥] and
Jeremy K. Nicholson^{||}

*Merck Sharp & Dohme Research Laboratories, The Neuroscience Research Centre,
Terlings Park, Harlow, Essex CM20 2QR, United Kingdom, Department of Safety Assessment,
Merck Research Laboratories, West Point, Pennsylvania 19486, Division of Biomedical Sciences,
Imperial College of Science, Technology and Medicine, Sir Alexander Fleming Building,
London SW7 2AZ, United Kingdom, and Department of Medicinal Chemistry, Merck Research
Laboratories, Rahway, New Jersey 07065*

Received June 19, 2003

An increased diversity of therapeutic targets in the pharmaceutical industry in recent years has led to a greater diversity of toxicological effects. This, and the increased pace of drug discovery, leads to a need for new technologies for the rapid elucidation of toxicological mechanisms. As part of an evaluation of the utility of metabonomics in drug safety assessment, ¹H NMR spectra were acquired on urine and liver tissue samples obtained from rats administered vehicle or a development compound (MrkA) previously shown to induce hepatotoxicity in several animal species. Multivariate statistical analysis of the urinary NMR data clearly discriminated drug-treated from control animals, due to a depletion in tricarboxylic acid cycle intermediates, and the appearance of medium chain dicarboxylic acids. High-resolution magic angle spinning NMR data acquired on liver samples exhibited elevated triglyceride levels that were correlated with changes in the urinary NMR data. Urinary dicarboxylic aciduria is associated with defective metabolism of fatty acids; subsequent *in vitro* experiments confirmed that MrkA impairs fatty acid metabolism. The successful application of metabonomics to characterize an otherwise ill-defined mechanism of drug-induced toxicity supports the practicality of this approach for resolving toxicity issues for drugs in discovery and development.

Introduction

The nascent sciences of genomics, proteomics, and metabonomics are attracting increasing attention from the pharmaceutical industry, since they offer the potential for earlier identification of compounds that are likely to fail for toxicological reasons and may provide a suite of tools by which toxicological mechanisms can be more rapidly elucidated (*1*). For example, where novel compound classes cause unusual types of toxicity or act via poorly understood mechanisms, a failure to resolve such problems quickly leads to compound attrition. Each of the “omic sciences” examines a different tier of biomolecular organization of an organism’s response to insult or pharmacology. Here, we focus on metabonomics, the characterization of the way in which the relative concentrations of endogenous small molecule components of

biofluids and tissues of complex organisms vary over time (*2, 3*).

The primary goals of metabonomics are to identify metabolic biomarkers associated with a specific biochemical event and to relate these to mechanism of effect. Variations in one or more endogenous metabolites may be associated with, and characteristic of, a pharmacological or toxicological event. For example, concurrent changes in more than 10 separate constituents of urine are together sufficient to distinguish renal papillary damage from renal tubular toxicity in rats (*4*). A substantial body of research has determined the metabonomic consequences on biofluids and target organs from animals dosed with prototypical toxins (*5*). However, relatively few reports have been published in which metabonomics has been applied in drug discovery, presumably reflecting the proprietary nature of pharmaceutical research. Three notable examples stand out. First, a variety of compounds that cause phospholipidosis all increased urinary excretion of phenylacetylglutamine (*6, 7*). Second, the antidiabetic efficacy of BRL 49653, a potent insulin-sensitizing agent, has been demonstrated in an animal model of diabetes mellitus by metabonomic evaluation of urine (*8*). Finally, Robertson et al. have described an metabonomic signature for vasculitis induced by phosphodiesterase type 4 inhibitors (*9, 10*). Although metabonomics is the newest of the omic sciences, it is particularly attractive because

* To whom correspondence should be addressed. Tel: +44(0)1279 440464. Fax: +44(0)1279 440390. E-mail: russell_mortishire-smith@merck.com.

[†] Merck Sharp & Dohme Research Laboratories, The Neuroscience Research Centre.

[‡] Present address: Bristol-Myers Squibb Company, Biotransformation, Princeton, NJ 08543.

[§] Department of Safety Assessment, Merck Research Laboratories.

^{||} Division of Biomedical Sciences, Imperial College of Science, Technology and Medicine.

[⊥] Department of Medicinal Chemistry, Merck Research Laboratories.

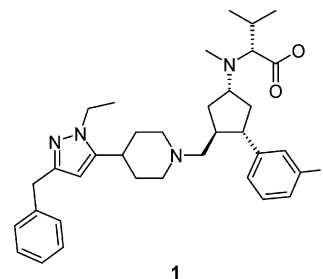
it has relatively low per sample costs, is often noninvasive, and uses technology that is widely available. Furthermore, changes that identify mechanism can be relatively easily used as biomarkers in screening assays for selection and development of compounds designed to circumvent toxicity.

^1H NMR spectra of biological fluids provide information on the relative concentrations of a wide variety of endogenous metabolites. To reduce the interpretational challenge presented by such large data sets, a strategy of data reduction followed by multivariate analysis techniques, such as PCA,¹ is typically employed (4). PCA combines correlated changes in many variables into a much smaller set of new orthogonal variables (PCs) while maintaining a maximal amount of variability from the original data (11). This permits the visualization of data in two or three dimensions and the detection of separation or clustering due to biochemical, genetic, or toxicological effects.

Intact tissues have historically been relatively intractable to analysis by NMR spectroscopy, primarily due to the constrained motion of the molecular species in the sample, which causes a pronounced broadening of the NMR spectrum. More recently, NMR spectra with improved resolution of intact tissues have been obtained using MAS NMR spectroscopy (12–15). Resonance broadening effects from dipolar coupling and chemical shift anisotropy scale with the function $(3\cos^2\theta - 1)/2$, which reduces to zero when the sample is oriented at an angle of 54.7° to the magnetic field. Spinning of the sample to mechanically induce “tumbling” of the low molecular weight species within the magnetic field further reduces broadening effects. These techniques yield NMR spectra of a resolution and dispersion comparable with that obtained from biological fluids.

Here, we describe the use of these techniques to investigate the mechanism of hepatotoxicity induced by a drug development candidate. MrkA (**1**, N-[3-[[4-(3-benzyl-1-ethyl-1H-pyrazol-5-yl)piperidin-1-yl]methyl]-4-(3-fluorophenyl)cyclopentyl]-N-methylvaline) is a selective chemokine receptor 5 receptor antagonist that was under development as an adjuvant HIV therapy (16, 17). In preparation for clinical studies, MrkA was first evaluated in 2 week oral toxicity studies in monkey and rats. Following 2 weeks of administration to monkeys at 10, 30, and 100 mg/kg/day, mild to moderate serum transaminase (ALT/AST) increases occurred at doses of 100 mg/kg/day. Five of the eight animals at that dose exhibited ALT increases that were greater than the 95% confidence interval for an historical set of control animal data. The mean ALT value at that dose was increased by 78% relative to concurrent controls. AST levels were higher than pretest values in seven of the eight animals with an overall mean increase of 47%. Pretest and control ALT and AST levels were all within the normal range for historical data. Moreover, these changes correlated with granular centrilobular hypertrophy and, in some animals, hepatic single cell necrosis (four of eight) and acute cholangitis (three of eight). In a corresponding rat study, there was only a slight increase in liver weights

at the high dose with no associated histopathological findings. However, subsequent experiments demonstrated that under certain conditions the toxicity could also be reproduced in rats, which provided a convenient model in which to investigate the mechanism of toxicity.



Together, these observations were indicative only of a nonspecific hepatotoxicity of sufficient severity to conclude that the compound could not be further developed. In vitro investigative studies were also conducted in precision-cut liver slices from rats and monkeys, and while toxicity was observed at relevant drug concentrations, no further insight into the mechanism was obtained. Because little was known about the possible toxicological consequences of CCR-5 inhibition, it was uncertain whether the observed toxicity was “mechanism-based” (due to the intended pharmacological mechanism of the drug) or an untoward off-target related feature of the compound. The viability of CCR-5 knockout mice (18) and the observation that CCR-5 is polymorphically expressed in humans (19, 20) were consistent with the latter hypothesis.

The distinction of mechanism-based from nonmechanism-based toxicity is important since the latter can, in principle, be designed out of a molecule. At the current pace of drug discovery and development, the rational design of a new molecule based on elucidation of the mechanism of toxicity requires a more rapid determination of the mechanism than is often practical using conventional toxicological techniques. This issue is one of the principal factors driving the development of new technologies, and the potential for rapidly identifying the mechanism of MrkA toxicity led us to conduct metabolic studies.

Experimental Section

Materials. HPLC grade laboratory chemicals were obtained from Sigma-Aldrich.

In Vivo Studies. Rats (CrI:CD (SD)IGS BR; ca. 6 weeks of age) and mice (CrI:CD-1 (ICR) BR; ca. 40 days of age) were obtained from Charles River, and Rhesus monkeys (*Macaca mulatta*; ca. 2–3 years of age) were obtained from New Iberia Research Center. All animal husbandry procedures were in accordance with the Guide for the Care and Use of Laboratory Animals (NIH Publication, Volume 25, Number 28, August 16, 1996, <http://grants1.nih.gov/grants/guide/notice-files/not96-208.html>), and all experimental procedures were approved by Institutional Animal Care and Use Committees (IACUC) of the facilities in which the studies were conducted. All animals were housed in standard laboratory animal facilities and were provided free access to water and, except during urine collection, measured amounts of food.

MrkA was administered orally as an aqueous suspension in 0.5% methylcellulose. Administration was once per day by gavage in volumes of 5 mL/kg. Control animals received aqueous 0.5% methylcellulose only. Two investigative studies were

¹ Abbreviations: ALT, alanine-aminotransferase; AST, aspartate-aminotransferase; DMSO, dimethyl sulfoxide; HIV, human immunodeficiency virus; LDH, lactate dehydrogenase; MAS, magic angle spinning; MCDA, medium chain dicarboxylic acid; MCAD, medium chain acyl-CoA dehydrogenase; PCA, principal components analysis; PC, principal component; TSP, trimethylsilylpropionic acid.

conducted in rats. In the first study (study A), doses of 0 (control) and 500 mg/kg/day were planned to be administered for 2 weeks to 15 animals per sex in each dose group. After four doses, urine was collected for metabonomic analysis and the study was terminated due to excessive toxicity and mortality. A second 2 week study (study B) was conducted at doses of 0 (control), 100, and 250 mg/kg/day for a planned 2 week study. Urine and plasma were scheduled for collection from all rats in study B after 1, 4, 7, and 14 doses. Early termination of some dose groups was also necessary in this study because of excessive toxicity. In both studies, in animals terminated early, clinical chemistry samples were obtained at termination. Liver samples were obtained for histological and metabonomic evaluation at termination, scheduled or otherwise.

When urine was collected for metabonomic analysis, animals were placed in metabolism cages and food was removed to prevent contamination of the urine. This procedure effectively resulted in a fast during the entire urine collection period. Urine was collected overnight (18 h) directly over dry ice from subsets of animals before and after various lengths of drug treatment or at the end of the study. In some cases, animals were terminated immediately after urine collection and liver samples were collected to correlate urinary metabonomic findings with histopathologic and metabonomic analysis of the liver. Urine and tissue samples obtained for metabonomic analysis were stored at -70°C . For histopathological evaluation, tissue was fixed in 10% neutral buffered formalin, prepared by routine methods, and stained with hematoxylin and eosin for microscopic evaluation and with oil red-O for the potential presence of lipids in vacuoles.

In Vitro Studies. Naïve male rats were anesthetized with isoflurane, and after exsanguination, their livers were removed and placed in ice-cold Krebs–Henseleit buffer (pH 7.4). Cores of tissue (0.8 cm diameter) obtained with a Tissue Coring Press (Alabama Research and Development Corporation) were precision cut (ca. 300 μm thickness) with a Krumdieck Liver Slicer (Alabama Research and Development Corporation).

Toxicity Experiments. Liver slices were placed in vials designed to ensure proper exposure to oxygen and incubated in 1.4 mL of Waymouth's MB752/1 medium (pH 7.4) supplemented with 25 mM HEPES, 25 mM NaHCO_3 (pH 7.4), 10% fetal bovine serum, 16.8 $\mu\text{g}/\text{mL}$ gentamicin, 2.5 mg/mL fungizone (amphotericin B), 5 μM dexamethasone, and 0.15 IU/mL insulin. Incubations were conducted at 37°C under a 95:5 O_2/CO_2 atmosphere. After a 45 min preincubation, the medium was replaced with fresh medium supplemented with various concentrations of MrkA introduced in DMSO (final DMSO concentration, 0.5–1.0%). After incubation for 24 or 48 h, LDH in the medium was measured with a commercially available kit (Sigma Chemical Co. catalog no. 228-20). For measurement of intracellular ATP and GSH, slices were homogenized in 0.5 mL of 10% perchloric acid and then centrifuged to obtain the supernatant. A portion (0.4 mL) of the supernatant was treated with 0.09 mL of 8 N KOH to precipitate the perchloric acid and then buffered with 0.1 mL of KH_2PO_4 (1.5 M, pH 6.0). After centrifugation, the supernatant was analyzed as described by Stocchi et al. (21) to quantify ATP. The total, nonprotein sulfhydryl (GSH) content of the supernatant was measured as described by Ellman (22). For measurement of protein synthesis, slices were pulse treated with [^3H]leucine (0.3 $\mu\text{Ci}/\text{mL}$) and incubated for an additional 2 h after which the leucine incorporation was quantified as described by Smith et al. (23). The protein content of the liver slices was measured as described by Lowry et al. (24).

Fatty Acid Oxidation Experiments. Slices ($n = 3/\text{treatment}$) were preincubated at 37°C on a Forma Scientific Orbital Shaker at 110 rpm in 24 well culture plates with 0.5 mL of Waymouth's 752/1 medium (pH 7.4) supplemented as described above. Preincubations included MrkA at various concentrations or etomoxir at 3 μM introduced in 0.5 or 1.0% DMSO. Control samples contained only DMSO. After the preincubation, the

medium was removed and replaced with 0.5 mL of fresh medium including drug (vide supra) and 30 μM [^3H]palmitic acid (1.17 $\mu\text{Ci}/\mu\text{mol}$; NEN) and incubated for an additional 4 h as described above. The slices were then removed and sonicated with a Fisher Sonic Dismembrator model 300 in 200 μL of 35% perchloric acid and 500 μL of phosphate-buffered saline. After they were incubated in ice-cold water for 10 min, the samples were centrifuged at 17 500g for 5 min and filtered (Millipore Filter System, MADVN6510), and the filtrate was counted in 10 mL of Ready Safe Scintillation Cocktail (Beckman) on a LS6000SC Scintillation Counter (Beckman).

Preparation of NMR Samples and NMR Data Collection. Urinary NMR samples were prepared by buffering 1 mL of raw urine with 0.5 mL of 0.2 M phosphate, centrifuging at 7000g for 10 min, and then transferring 200 μL aliquots of supernatant into a 96 well plate, and adding 20 μL of a 10 mM solution of TSP in D_2O subsequently to each well. One-dimensional (1D) ^1H NMR spectra were acquired on a Bruker DPX-400 NMR spectrometer equipped with a 4 mm flow probe and Gilson 215 autosampler. Following transfer of 175 μL of each sample into the flow cell, data were acquired at 400 MHz into 32K points using a spectral width of 5200 Hz, a 1D noesy-preset pulse sequence with a relaxation delay of 1.5 s, mixing time of 100 ms, and 128 transients per sample. Sample temperatures were maintained at 300 K.

For MAS NMR analysis of liver tissue, samples (~ 10 mg) were placed into a 4 mm zirconium oxide rotor to which a single drop of D_2O had been added to act as field frequency lock. The rotor was inserted into a high-resolution MAS NMR probe on a Bruker DPX 400 spectrometer and spun at frequencies between 2000 and 8000 Hz. The sample temperature was regulated at 278 K following calibration of the probehead temperature at the selected spin speed (25). All spectra were acquired using standard methods of water suppression. Conventional ^1H NMR spectra were acquired using 128 scans into 64K data points over a spectral width of 6410 Hz with an acquisition time of 2.55 s and a total pulse recycle delay of 5.56 s. Carr–Purcell–Meiboom–Gill 1D ^1H NMR spectra were acquired using 256 scans into 64K data points over a spectral width of 6410 Hz with a spin–echo time of 80 ms. Double quantum filtered correlation (DQF-COSY), total correlation (TOCSY, 150 ms mixing time), heteronuclear single quantum correlation (HSQC), and heteronuclear multiple bond correlation (HMBC) experiments were acquired using standard pulse sequences. Typically, for each experiment, 512 increments of 2K data points were acquired with 32 scans per increment and a ^1H spectral width of 8000 Hz.

NMR Data Analysis. One-dimensional NMR data were subjected to 0.15 Hz exponential line broadening, Fourier transformed, phase corrected, and baseline optimized, and then prepared for analysis by reducing the 10 to -0.2 ppm region down to 256 buckets each of 0.04 ppm using the software package AMIX (version 2.7, Bruker Analytische Messtechnik, Rheinstetten, Germany). Regions of the spectrum containing resonances from residual water or urea were removed prior to analysis. The resulting bucketed urinary spectra were normalized for concentration by dividing the intensity of each bucket by the total integral of the spectrum. Multivariate statistical analyses were performed using Pirouette (v 3.02, Infometrix Inc., Woodinville, WA), mean centering data prior to PCA.

Results

In Vivo Toxicological Findings. In the first investigative study in rats (study A), nine females and two males in the 500 mg/kg/day group died after urine collection on the 5th day of the study. Substantial increases in mean transaminase values (ALT and AST) were seen in drug-treated females (5.1- and 3.6-fold), whereas less severe increases were seen in drug-treated males (1.4- and 1.6-fold), relative to controls. Pretest

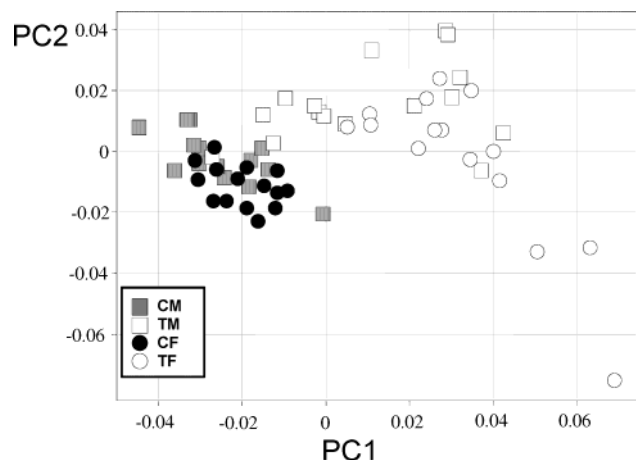


Figure 1. First two PCs obtained by PCA on all 60 drug day 4 samples, classified by gender and dose group.

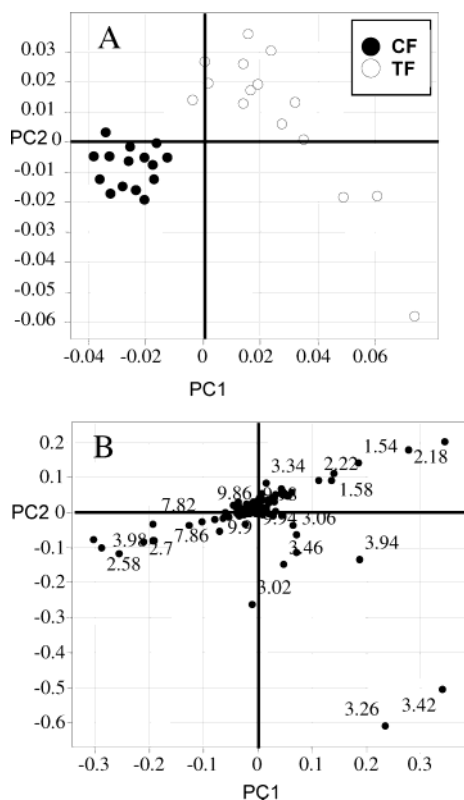


Figure 2. (A) PC1 v PC2 for female control (CF) and female dosed (TF) drug day 4 urine samples. (B) Loadings plot for panel A (comparison of CF and TF animals), highlighting resonances at 1.54, 2.18, and 1.30 ppm as primary contributors to the discrimination between CF and TF groups and resonances at 3.26 and 3.42 ppm dominating the variance within the TF group.

serum chemistry values were not obtained, but control values for both ALT and AST were within the normal limits of an historical data set for the same species and strain of rat. At gross examination, an increase in mean liver weight (adjusted for body weight) was seen in drug-treated males and females (50 and 90%, relative to controls) and corresponded with liver pallor in both sexes. Upon histopathological examination of the liver, hepatocellular vacuolation was seen in all drug-treated animals (15/sex). Approximately half of all drug-treated animals also had hepatic single cell necrosis, focal necrosis, and/or neutrophilic infiltration.

In the second 2 week study in rats (study B, with doses of 100 and 250 mg/kg/day), eight of 15 females in the 250

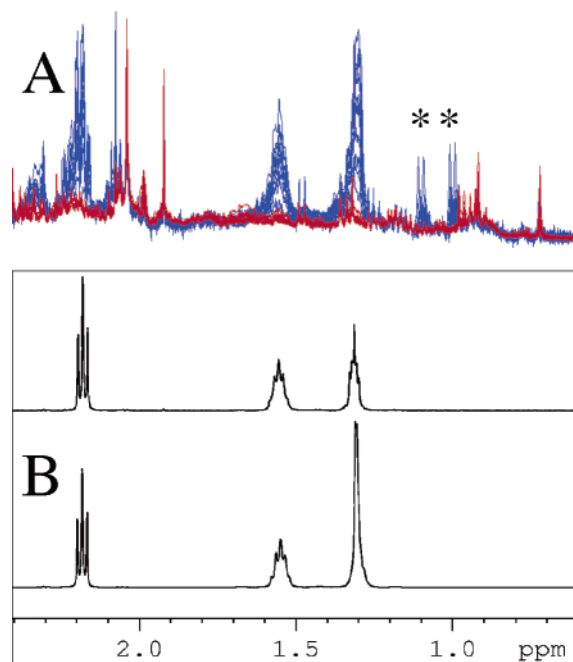


Figure 3. (A) Comparison of high field regions of the NMR spectra from CF (red) and DF (blue) rats. Starred resonances derive from excreted MrkA. (B) Reference spectra of analytical grade suberic (middle) and sebacic (bottom) acid.

mg/kg/day group died the evening after the first dose during the 18 h fast necessitated by urine collection for metabonomic analysis. Surviving rats in the 250 mg/kg/day group were subsequently sacrificed and necropsied. For comparative purposes, a subset of animals in the control and 100 mg/kg/day groups (five/sex) were also sacrificed after the second dose and necropsied and samples were collected for analysis. Following the first dose, mean ALT values in the 250 mg/kg/day group were increased 8.9- and 2.8-fold in female and male rats, respectively. In the 100 mg/kg/day group, the mean ALT value for females was increased approximately 4.1-fold following the first dose, whereas ALT values were unaffected in male rats at this dose. On subsequent days, there were no effects on ALT values in females or males in the 100 mg/kg/day group. At gross examination, increased liver weights (adjusted for body weight) were seen in both sexes in the 100 and 250 mg/kg/day groups and corresponded with liver pallor. Upon histological examination, hepatocellular vacuolation was seen in both sexes in the 100 and 250 mg/kg/day groups and corresponded with the gross findings.

Metabonomic Characterization of Urine. NMR data were acquired on urine samples collected on drug day 4 of study A in which 30 male and 30 female rats were administered either 500 mg/kg/day of MrkA or vehicle (yielding 15 animals per dose/gender group). The resulting NMR spectra were reduced to 256 intensity variables of 0.04 ppm each, normalized by expressing the intensity of each variable as a fraction of the total intensity for the spectrum, mean centered, and subjected to PCA. Initial inspection of the NMR spectra and comparison of the latter with the NMR spectrum of MrkA revealed that the urinary excretion of MrkA and related metabolites was relatively low and had a minimal contribution to the observed variance between samples (however, regions containing identifiable drug resonances were subsequently excluded from the input data set).

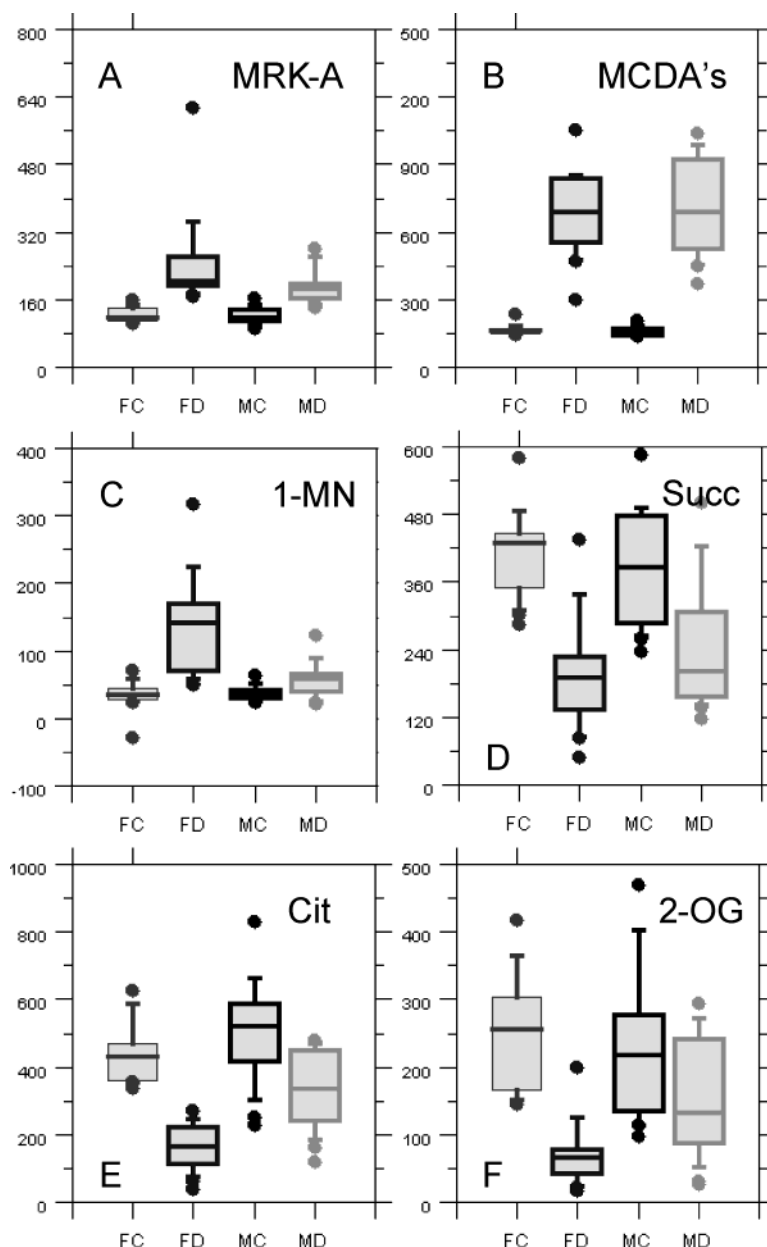


Figure 4. Box plots indicating substantive differences in metabolite excretion between groups, obtained by measuring the integral of a single, resolved resonance from each metabolite. The center line denotes the median value, the box represents the ranges of the 25–75th centiles, and the outer line represents the 10–90th centiles. The outer circles denote the total range of the data. (A) MrkA, (B) suberic/sebacic/pimelic acids, (C) 1-methylnicotinamide, (D) succinate, (E) citrate, and (F) 2-oxoglutarate. The Y-axis is scaled independently for each component.

Figure 1 shows a plot of the first two PCs for all 60 samples in study A, accounting for 69% of total variance, classified as CM (control male), TM (treated male), CF (control female), and TF (treated female). A clear discrimination of treated from control animals is evident. The separation of TF from CF samples is somewhat greater than the separation of TM from CM and correlates with the increased mortality, greater transaminase (AST/ALT), and liver weight increases seen in drug-treated females, relative to males.

To remove residual variation due to gender differences, the PCA was recalculated for the 30 spectra obtained for treated and CF animals only (Figure 2A). Inspection of the corresponding loadings plot (Figure 2B) highlights those resonances in the NMR spectra responsible for the separation of samples. Treated and control groups are separated from one another in PC1, with increases in the intensities of resonances at 1.30–1.34,

1.54–1.58, and 2.18–2.22 ppm and decreases in the intensities of resonances at 7.82–7.86, 2.42–2.66, and 3.98, among others, contributing substantially to variations in PC1. Interpretation of these data was as follows, accomplished by inspection of the original NMR spectra. Three TF animals clustering toward the bottom right of the scores plot exhibited elevated levels of taurine (3.26 and 3.42 ppm). Citrate, succinate, 2-oxoglutarate, and hippurate were depleted in urine from treated animals of both sexes but with more pronounced depletions in females. On inspection, 1-methylnicotinamide was also identified as being increased approximately 3-fold in TFs but was not significantly increased in TMs.

Changes in the NMR spectra of treated animals at 1.30–1.34, 1.54–1.58, and 2.18–2.22 ppm were remarkable in that they indicated the excretion of novel nonendogenous species—a comparison of these regions of the

NMR spectra for treated and control animals is shown in Figure 3A. A directed search of library data using AMIX with SBASE 1.1.2 indicated that two MCDAs, sebacic and suberic acids, had chemical shifts consistent with the novel species observed in treated animals (Figure 3B). Pimelic acid, although not contained in SBASE 1.1.2, has a similar NMR spectrum. These dicarboxylic acids have closely related NMR spectra, but NMR spectroscopy cannot easily determine their relative concentrations. Two-dimensional homonuclear (DQF-COSY, TOCSY) and heteronuclear (HSQC, HMBC) experiments were acquired on a typical urinary sample and on authentic reference standards to confirm the assignment of these proton resonances as MCDAs. These data were entirely consistent with the presence of a mixture of suberic, sebacic, and/or pimelic acids. Qualitatively, one or all were present in the urine from treated animals. None are normally present in urine from healthy animals but are typically observed as a consequence of impaired fatty acid metabolism. A comparison of the relative levels of selected urinary components in treated and control, male and female animals is shown in Figure 4, calculated by measurement of the peak area (arbitrary units) of a resolved resonance for each component.

Metabonomic Characterization of Liver Tissue.

MAS ^1H NMR spectra were acquired at 400 MHz on liver tissue taken at sacrifice from male rats treated for 2 days with vehicle ($n = 5$), MrkA at 100 ($n = 4$, day 2) or 250 mg/kg/day ($n = 5$), or 15 days with vehicle ($n = 5$) or MrkA at 250 mg/kg/day ($n = 5$) (study B). Spectra were normalized relative to the trimethylamine oxide/betaine resonance envelope at 3.26 ppm. Solution ^1H NMR spectra were also collected on urine samples obtained prior to sacrifice. Figure 5A shows representative 400 MHz MAS ^1H NMR spectra of liver tissue samples from animals treated for 2 days with vehicle, 100, or 250 mg/kg/day MrkA. The levels of glycogen and α/β -glucose in control samples were substantially lower (and in some cases, below the limit of detection) as compared with other literature reports (26), presumably because animals were fasted prior to urine collection. All of the assigned triglyceride resonances (26) were seen in the NMR spectra of control samples; however, the broad resonance (or resonances) at 2.81 ppm was only seen in the NMR spectra of samples from treated animals. The relative levels of triglycerides in the NMR spectra (as judged by the peak area of the resonance at 1.30 ppm relative to the resonance envelope at 3.26 ppm assigned to trimethylamine oxide/betaine) are shown in Figure 5B. After 2 days dosing with MrkA at 100 mg/kg/day, triglyceride levels, as judged by MAS NMR, were not significantly elevated, while at 250 mg/kg/day an approximate 10-fold increase in liver triglycerides was noted. By day 15, liver triglyceride levels in animals treated at 100 mg/kg/day showed an approximate 5-fold increase over controls. The relationship between urinary MCDA excretion (as judged by the intensity of the resonance envelope at 1.54 ppm) and levels of liver triglycerides at sacrifice (as judged by the intensity of the resonance envelope at 1.30 ppm) is shown in Figure 5C (27). While liver triglyceride levels were not significantly elevated by day 2 at 100 mg/kg/day, urinary excretion of MCDAs at this dose level showed a 2-fold increase. By day 15, urinary MCDA excretion had returned to control levels in 100 mg/kg/day treated animals, while liver triglycerides were now slightly elevated (1.3-fold increase). Interestingly, the 250

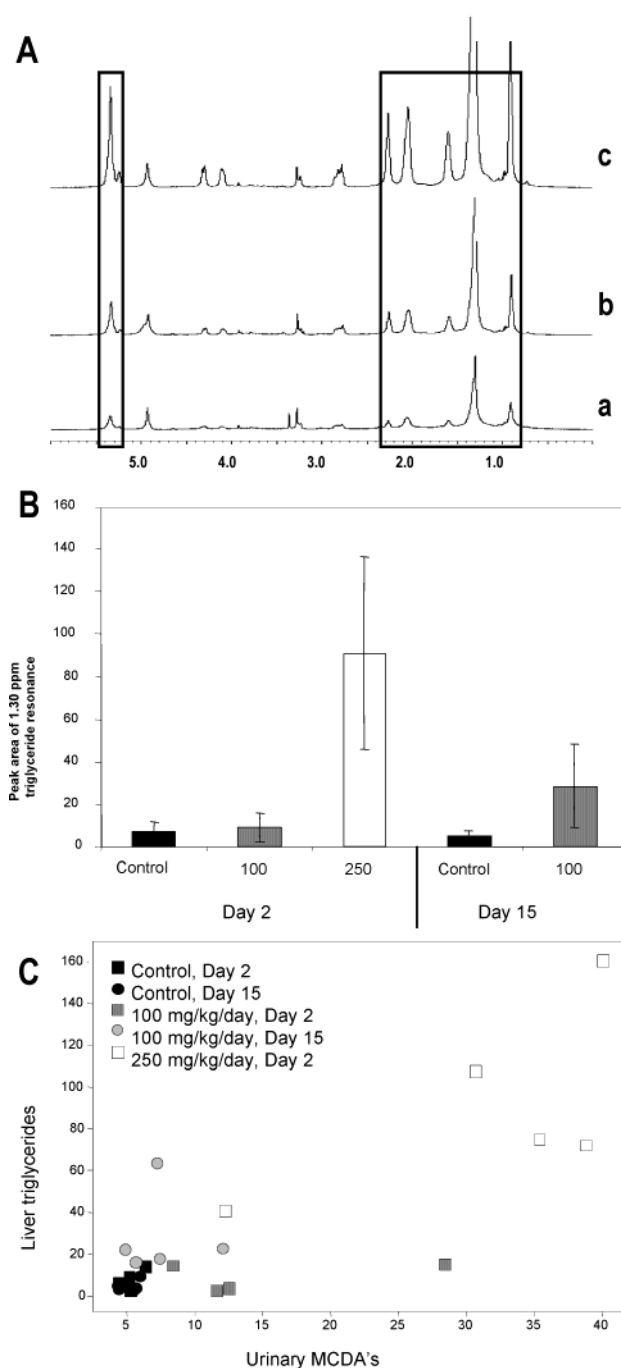


Figure 5. (A) Comparison of ^1H HR-MAS NMR data acquired on liver tissue taken from rats dosed with MrkA at (a) 0, (b) 100, and (c) 250 mg/kg/day for 2 days. (B) Dose dependency of triglyceride levels (peak area of 1.30 ppm resonance envelope) on days 2 and 15 (mean \pm 1 SD). (C) Relationship between liver triglyceride and urinary MCDA levels (peak area measurements for selected resolved resonances) determined from tissue and urinary ^1H NMR data.

mg/kg/day animal showing the smallest increase in liver triglycerides exhibited concomitantly low urinary MCDA excretion.

In Vitro Toxicological Studies with MrkA. In vitro assessment of MrkA toxicity in precision-cut liver slices, as determined by traditional measures of cell viability (LDH leakage, protein synthesis, and intracellular ATP and GSH concentrations), indicated that MrkA was toxic at concentrations similar to those associated with toxicity in vivo (Figure 6A). Concentrations of MrkA in the livers of rats treated with MrkA at 250 mg/kg/day ranged

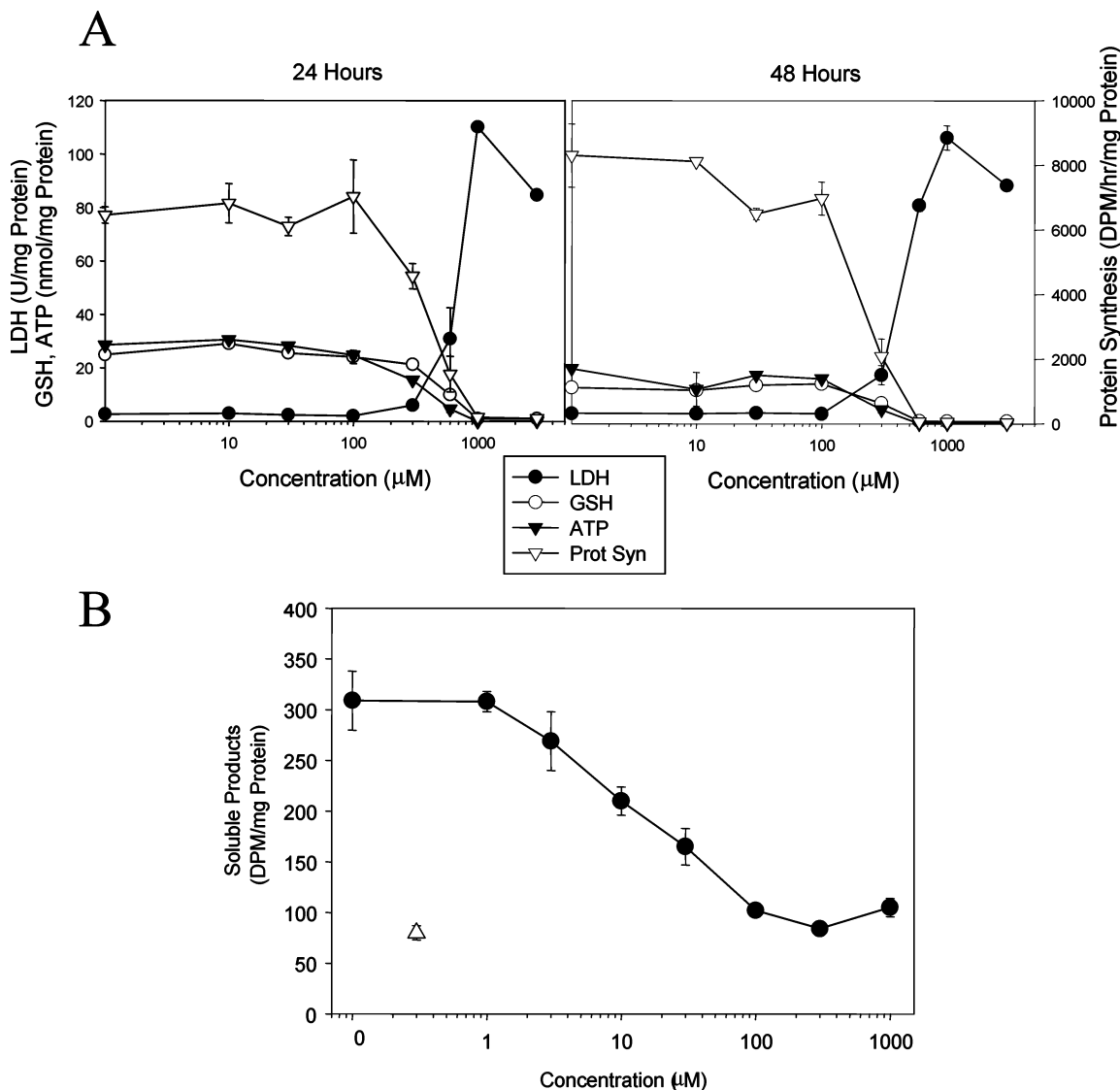


Figure 6. In vitro toxicity of MrkA measured in rat liver slices. (A) LDH (●) released into the culture medium, and intracellular GSH (○), ATP (▼), and protein synthesis (▽) after 24 and 48 h incubations. (B) Chain shortening of $[^3\text{H}]$ palmitate after incubation for 4 h with MrkA (●) and a single concentration of etomoxir (⊗) as a positive control. Error bars show standard deviation of three measurements.

between 50 and 300 μM . The in vitro toxicity was shown to be concentration- and modestly time-dependent; however, these limited end points did not reveal clues about the possible mechanism of toxicity. After the metabonomic results were obtained, additional histopathological results from subsequent studies at higher doses showed oil red-O positive vacuolation in the liver of rats treated with MrkA, possibly due to a steatosis resulting from the disruption of fatty acid metabolism. The observation in the in vivo studies that fasting caused histopathological changes at doses where there was little or no effect in nonfasted animals treated with MrkA further substantiated inhibition of fatty acid metabolism as the mechanism of toxicity (vide supra). Inhibition of fatty acid oxidation might have been expected to cause a more distinct effect on ATP concentrations in the liver slice studies, but high concentrations of glucose and other sources of energy (necessary to sustain viable slices) may have maintained ATP despite inhibition of fatty acid metabolism.

The ability of MrkA to directly inhibit fatty acid oxidation was evaluated to confirm the metabonomic findings. The β -oxidation of $[^3\text{H}]$ palmitic acid in the

absence and presence of MrkA was studied in precision-cut liver slices prepared from naïve rats. Soluble palmitate products (chain shortened by β -oxidation) were measured after a 4 h incubation of 30 μM $[^3\text{H}]$ palmitic acid and various concentrations of MrkA (Figure 6B), using a concentration of etomoxir known to inhibit chain shortening, as a positive control (28). Inhibition of fatty acid oxidation occurred at concentrations of MrkA substantially lower than those associated with overt toxicity, a distinction that is expected when comparing specific and general end points. The differences were not due to variations in the concentrations of free vs protein-bound drug in the incubation medium since differences in free drug in the two assays were small (ca. 2-fold, data not shown) as compared to the difference between inhibition of β -oxidation and toxicity (ca. 20-fold). Additional studies demonstrated that MrkA inhibited β -oxidation of palmitoyl-CoA and palmitoyl-carnitine in isolated liver mitochondria (data not shown).

Discussion

The initial in vivo toxicological findings provided no insight into the mechanism of toxicity caused by MrkA.

These results only showed toxicity of sufficient severity to warrant termination of the development of the compound. Only with the subsequent investigative in vivo studies in rats was a toxicity associated with fasting indicated. Indeed, this observation correlated with the metabolomic findings and served to corroborate a finding of disruption of fatty acid utilization. When rats fed ad libitum were dosed at 100 mg/kg/day, they survived for 2 weeks with no signs of toxicity. In another study at the same dose, when rats were fasted during the course of the study, severe toxicity ensued. At a higher dose of 250 mg/kg/day, animals survived for 5 days when they were not fasted but mortality occurred after a single dose with fasting. These observations indicated a possible perturbation of energy utilization that correlated with the metabolomic findings.

Depletions in urinary excretion of the tricarboxylic acid cycle intermediates citrate, 2-oxoglutarate, and succinate are consistent with an increased cellular energy demand. By themselves, these changes do not unambiguously identify the toxicological event specific to the liver nor do they indicate any specific mechanism of toxicity. A useful general marker of hepatotoxicity is taurinuria (29), and a small number of MrkA-treated females exhibited elevated levels of urinary taurine. 1-Methylnicotinamide synthesis has been shown to be upregulated (ca. 2–4-fold higher) in both regenerating liver and thioacetamide-treated liver slices as compared with control slices (30). Perturbations in urinary hippurate excretion during metabolomic studies have been previously noted and are often associated with changes in feeding regimes (31, 32). The concerted relative changes in excretion of these endogenous metabolites may be sufficient to define a unique metabolomic profile for the hepatotoxicity, but by themselves, they do not identify the mechanism of toxicity observed with MrkA.

A specific mechanism for the observed hepatotoxicity of MrkA is suggested by the appearance of MCDAs. These components are not normal constituents of urine; their appearance is typically associated with defective fatty acid metabolism, specifically the inhibition of early steps in the β -oxidation pathway. For example, MCAD deficiency, an inborn error of metabolism, is characterized by the detection of dicarboxylic and hydroxy acids derived from ω -oxidation and ω -1 oxidation, respectively, of accumulating monocarboxylic acids (33–35). The tetrahydropyridine analogue of haloperidol causes elevation of urinary dicarboxylic acids in the baboon, and this is considered to be a consequence of a defect in mitochondrial respiration (36). The hepatotoxic component (hypoglycin A) of the unripe Jamaican ackee fruit also causes profound hypoglycemia, depletion of liver glycogen, and an associated dramatic increase in the excretion of dicarboxylic acids such as ethylmalonic, glutaric, sebacic, and suberic acids (37).

Histological changes seen in the livers of rats treated with MrkA at 500 mg/kg/day were consistent with those seen in patients with MCAD deficiency (specifically, hepatomegaly with micro- or macrovesicular lipid accumulation) (38). Patients with MCAD deficiency and individuals exposed to hypoglycin A suffer exacerbated symptoms during conditions of fasting and hypoglycemia, due to their inability to shift metabolism from use of glucose to fatty acids. In this regard, it is notable that we observed increased mortality of MrkA-treated animals during the fasting conditions used for urine collection.

Steatosis is not always associated with the degree of toxicity observed here nor does it necessarily indicate that toxicity is due to impairment of fatty acid oxidation. However, in the case of MrkA, the combination of the metabolomic findings, the association of toxicity with fasting, and the demonstrated potent in vitro inhibition of fatty acid oxidation are consistent with the conclusion that MrkA toxicity was due directly to an impaired β -oxidation pathway.

Conclusion

Characterization of the urinary metabolome was the key step in rapidly ascertaining the likely mechanism of toxicity and led to the development of appropriate in vivo and in vitro experiments confirming that MrkA impaired fatty acid metabolism. Further studies on other compounds in comparable situations are needed to determine how substantial the role of metabolomics will be in drug development and discovery.

Acknowledgment. We are grateful to John Lindon for helpful discussions. A.W.N. was supported by a Merck Senior Research Fellowship.

References

- (1) Hamadeh, H. K., Amin, R. P., Paules, R. S., and Afshari, C. A. (2002) An overview of toxicogenomics. *Curr. Issues Mol. Biol.* 4 (2), 45–56.
- (2) Shockcor, J. P., and Holmes, E. (2002) Metabolomic applications in toxicity screening and disease diagnosis. *Curr. Top. Med. Chem. (Hilversum, Netherlands)* 2 (1), 35–51.
- (3) Nicholson, J. K., Connelly, J., Lindon, J. C., and Holmes, E. (2002) Innovation: Metabolomics: a platform for studying drug toxicity and gene function. *Nat. Rev. Drug Discovery* 1 (2), 153–161.
- (4) Holmes, E., Nicholson, J. K., Nicholls, A. W., Lindon, J. C., Connor, S. C., Polley, S., and Connelly, J. (1998) The identification of novel biomarkers of renal toxicity using automatic data reduction techniques and PCA of proton NMR spectra of urine. *Chemom. Intell. Lab. Syst.* 44 (1, 2), 245–255.
- (5) Robertson, D. G., Reilly, M. D., Lindon, J. C., Holmes, E., and Nicholson, J. K. (2002) Metabolomic technology as a tool for rapid throughput in vivo toxicity screening. *Comprehensive Toxicol.* 583–610.
- (6) Espina, J. R., Shockcor, J. P., Herron, W. J., Car, B. D., Contel, N. R., Ciaccio, P. J., Lindon, J. C., Holmes, E., and Nicholson, J. K. (2001) Detection of in vivo biomarkers of phospholipidosis using NMR-based metabolomic approaches. *Magn. Reson. Chem.* 39 (9), 559–565.
- (7) Nicholls, A. W., Nicholson, J. K., Haselden, J. N., and Waterfield, C. J. (2000) A metabolomic approach to the investigation of drug-induced phospholipidosis: an NMR spectroscopy and pattern recognition study. *Biomarkers* 5 (6), 410–423.
- (8) Connor, S. C., Hughes, M. G., Moore, G., Lister, C. A., and Smith, S. A. (1997) Antidiabetic efficacy of BRL 49653, a potent orally active insulin-sensitizing agent, assessed in the C57BL/KsJ db/db diabetic mouse by noninvasive ^1H NMR studies of urine. *J. Pharm. Pharmacol.* 49 (3), 336–344.
- (9) Robertson, D. G., Reilly, M. D., Albassam, M., and Dethloff, L. A. (2001) Metabolomic assessment of vasculitis in rats. *Cardiovasc. Toxicol.* 1 (1), 7–19.
- (10) Slim, R. M., Robertson, D. G., Albassam, M., Reilly, M. D., Robosky, L., and Dethloff, L. A. (2002) Effect of dexamethasone on the metabolomics profile associated with phosphodiesterase inhibitor-induced vascular lesions in rats. *Toxicol. Appl. Pharmacol.* 183 (2), 108–109.
- (11) Wold, S., Geladi, P., Esbensen, K., and Oehman, J. (1987) Multiway principal components and PLS-analysis. *J. Chemom.* 1 (1), 41–56.
- (12) Waters, N. J., Garrod, S., Farrant, R. D., Haselden, J. N., Connor, S. C., Connelly, J., Lindon, J. C., Holmes, E., and Nicholson, J. K. (2000) High-Resolution Magic Angle Spinning ^1H NMR Spectroscopy of Intact Liver and Kidney: Optimization of Sample Preparation Procedures and Biochemical Stability of Tissue during Spectral Acquisition. *Anal. Biochem.* 282 (1), 16–23.

- (13) Garrod, S., Humpfer, E., Spraul, M., Connor, S. C., Polley, S., Connelly, J., Lindon, J. C., Nicholson, J. K., and Holmes, E. (1999) High-resolution magic angle spinning ^1H NMR spectroscopic studies on intact rat renal cortex and medulla. *Magn. Reson. Med.* 41 (6), 1108–1118.
- (14) Waters, N. J., Holmes, E., Waterfield, C. J., Farrant, R. D., and Nicholson, J. K. (2002) NMR and pattern recognition studies on liver extracts and intact livers from rats treated with α -naphthylisothiocyanate. *Biochem. Pharmacol.* 64 (1), 67–77.
- (15) Waters, N. J., Holmes, E., Williams, A., Waterfield, C. J., Farrant, R. D., and Nicholson, J. K. (2001) NMR and Pattern Recognition Studies on the Time-Related Metabolic Effects of α -Naphthyl isothiocyanate on Liver, Urine, and Plasma in the Rat: An Integrative Metabonomic Approach. *Chem. Res. Toxicol.* 14 (10), 1401–1412.
- (16) Farber, J. M., and Berger, E. A. (2002) HIV's response to a CCR5 inhibitor: I'd rather tighten than switch! *Proc. Natl. Acad. Sci. U.S.A.* 99 (4), 1749–1751.
- (17) De Clercq, E., and Schols, D. (2001) Inhibition of HIV infection by CXCR4 and CCR5 chemokine receptor antagonists. *Antiviral Chem. Chemother.* 12 (Suppl. 1), 19–31.
- (18) Sato, N., Kuziel, W. A., Melby, P. C., Reddick, R. L., Kostecki, V., Zhao, W., Maeda, N., Ahuja, S. K., and Ahuja, S. S. (1999) Defects in the generation of IFN- γ are overcome to control infection with *Leishmania donovani* in CC chemokine receptor (CCR) 5-, macrophage inflammatory protein-1 α , or CCR2-deficient mice. *J. Immunol.* 163 (10), 5519–5525.
- (19) Gonzalez, E., Dhand, R., Bamshad, M., Mummidi, S., Geevarghese, R., Catano, G., Anderson, S. A., Walter, E. A., Stephan, K. T., Hammer, M. F., Mangano, A., Sen, L., Clark, R. A., Ahuja, S. S., Dolan, M. J., and Ahuja, S. K. (2001) Global survey of genetic variation in CCR5, RANTES, and MIP-1 α : impact on the epidemiology of the HIV-1 pandemic. *Proc. Natl. Acad. Sci. U.S.A.* 98 (9), 5199–5204.
- (20) Carrington, M., Dean, M., Martin, M. P., and O'Brien, S. J. (1999) Genetics of HIV-1 infection: chemokine receptor CCR5 polymorphism and its consequences. *Hum. Mol. Genet.* 8 (10), 1939–1945.
- (21) Stocchi, V., Cucchiari, L., Canestrari, F., Piacentini, M. P., and Fornaini, G. (1987) A very fast ion-pair reversed-phase HPLC method for the separation of the most significant nucleotides and their degradation products in human red blood cells. *Anal. Biochem.* 167 (1), 181–190.
- (22) Ellman, G. L. (1959) Tissue sulphydryl groups. *Arch. Biochem. Biophys.* 82, 70–77.
- (23) Smith, P. F., Fisher, R., Shubat, P. J., Gandolfi, A. J., Krumdieck, C. L., and Brendel, K. (1987) In vitro cytotoxicity of allyl alcohol and bromobenzene in a novel organ culture system. *Toxicol. Appl. Pharmacol.* 87 (3), 509–522.
- (24) Lowry, O. H., Rosebrough, N. J., Farr, A. L., and Randall, R. J. (1951) Protein measurement with the Folin phenol reagent. *J. Biol. Chem.* 193, 265–275.
- (25) Nicholls, A. W., and Mortishire-Smith, R. J. (2001) Temperature calibration of a high-resolution magic-angle spinning NMR probe for analysis of tissue samples. *Magn. Reson. Chem.* 39 (12), 773–776.
- (26) Bollard, M. E., Garrod, S., Holmes, E., Lindon, J. C., Humpfer, E., Spraul, M., and Nicholson, J. K. (2000) High-resolution ^1H and ^1H - ^{13}C magic angle spinning NMR spectroscopy of rat liver. *Magn. Reson. Med.* 44 (2), 201–207.
- (27) Kose, F., Weckwerth, W., Linke, T., and Fiehn, O. (2001) Visualizing plant metabolomic correlation networks using clique-metabolite matrixes. *Bioinformatics* 17 (12), 1198–1208.
- (28) Spurway, T. D., Sherratt, H. S., Pogson, C., and Agius, L. (1997) The flux control coefficient of carnitine palmitoyltransferase I on palmitate β -oxidation in rat hepatocyte cultures. *Biochem. J.* 323 (1), 119–122.
- (29) Beckwith-Hall, B. M., Nicholson, J. K., Nicholls, A. W., Foxall, P. J. D., Lindon, J. C., Connor, S. C., Abdi, M., Connelly, J., and Holmes, E. (1998) Nuclear Magnetic Resonance Spectroscopic and Principal Components Analysis Investigations into Biochemical Effects of Three Model Hepatotoxins. *Chem. Res. Toxicol.* 11 (4), 260–272.
- (30) Hoshino, J., Kuehne, U., and Kroeger, H. (1982) Methylation of nicotinamide in rat liver cytosol and its correlation with hepatocellular proliferation. *Biochim. Biophys. Acta* 719 (3), 518–526.
- (31) Phipps, A. N., Stewart, J., Wright, B., and Wilson, I. D. (1998) Effect of diet on the urinary excretion of hippuric acid and other dietary-derived aromatics in rat: a complex interaction between diet, gut microflora and substrate specificity. *Xenobiotica* 28 (5), 527–537.
- (32) Phipps, A. N., Wright, B., Stewart, J., and Wilson, I. D. (1997) Use of proton NMR for determining changes in metabolite excretion profiles induced by dietary changes in the rat. *Pharm. Sci.* 3 (3), 143–146.
- (33) Gregersen, N., Mortensen, P. B., and Koelvraa, S. (1983) On the biologic origin of C6–C10-dicarboxylic and C6–C10- ω -1-hydroxy monocarboxylic acids in human and rat with acyl-CoA dehydrogenation deficiencies: in vitro studies on the ω - and ω -1-oxidation of medium-chain (C6–C12) fatty acids in human and rat liver. *Pediatr. Res.* 17 (10), 828–834.
- (34) Gregersen, N., Koelvraa, S., Rasmussen, K., Mortensen, P. B., Divry, P., David, M., and Hobolth, N. (1983) General (medium-chain) acyl-CoA dehydrogenase deficiency (nonketotic dicarboxylic aciduria): quantitative urinary excretion pattern of 23 biologically significant organic acids in three cases. *Clin. Chim. Acta* 132 (2), 181–191.
- (35) Rafter, J. E. M., Chalmers, R. A., and Iles, R. A. (1990) Medium-chain acyl-CoA dehydrogenase deficiency: a proton NMR spectroscopic study. *Biochem. Soc. Trans.* 18 (5), 912–913.
- (36) Mienie, L. J., Bergh, J. J., Van Staden, E., Steyn, S. J., Pond, S. M., Castagnoli, N., Jr., and Van der Schyf, C. J. (1997) Metabolic defects caused by treatment with the tetrahydropyridine analogue of haloperidol (HPTP), in baboons. *Life Sci.* 61 (3), 265–272.
- (37) Tanaka, K., and Ikeda, Y. (1990) Hypoglycin and Jamaican vomiting sickness. *Prog. Clin. Biol. Res.* 321, 167–184.
- (38) Saudubray, J. M., Martin, D., de Lonlay, P., Touati, G., Poggi-Travert, F., Bonnet, D., Jouvett, P., Boutron, M., Slama, A., Vianey-Saban, C., Bonnefont, J. P., Rabier, D., Kamoun, P., and Brivet, M. (1999) Recognition and management of fatty acid oxidation defects: a series of 107 patients. *J. Inherited Metab. Dis.* 22 (4), 488–502.

TX034123J